Periodic surfaces of simple and complex topology: Comparison of scattering patterns

Piotr Garstecki and Robert Hołyst
Institute of Physical Chemistry, PAS and College of Science, Department III, Kasprzaka 44/52, 01-224 Warsaw, Poland
(Received 27 September 2000; revised manuscript received 22 January 2001; published 11 July 2001)

We compute scattering patterns for six triply periodic minimal surfaces formed in oil/surfactant/water solutions: Three surfaces of a simple topology, Schwarz P ($Im\bar{3}m$), Schwarz D–diamond ($Pn\bar{3}m$), and Schoen G–gyroid ($Ia\bar{3}d$), and three surfaces of a complex topology, SCN1 ($Im\bar{3}m$), CD ($Pn\bar{3}m$), and GX6 ($Ia\bar{3}d$). We show that in the case of the complex structures, scattering intensity is shifted towards the higher hkl peaks. This might cause their misidentification and wrong estimates about the cell size of the structure.

DOI: 10.1103/PhysRevE.64.021501 PACS number(s): 68.05.−n

I. INTRODUCTION

The surfactant molecules are composed of a polar hydrophilic head and a hydrophobic hydrocarbon tail. This amphiphilic construction induces very complex behavior in solutions with water and oil. The surfactant molecules form layers that separate oil- and water-rich regions. In solutions with comparable concentration of surfactants and water, bicontinuous structures are formed. These can be either isotropic microemulsions in ternary systems (with oil and water) and sponge phases in binary systems (with water) or highly ordered cubic liquid phases of various symmetries. In both cases the surfactant layers are not planar or spherical but form complex three-dimensional structures free of self-intersections—triply periodic surface.

The cubic phases in self-aggregating surfactant systems have been observed experimentally many times in the last four decades. The first reports date back to 1967 (Luzzati and Spegt [1]). Since then several cubic phases with various symmetries and topologies have been discovered, see, for example, [2–7]. The latter references include experimental scattering data proving existence of all of the simple structures (Schwarz P, Schwarz D, and Schoen G) concerned in this paper. At the same time the existance of the complex structures (SCN1, CD, GX6) has not yet been confirmed. Still, new phases are being found and the list of the experimentally identified cubic phases may be incomplete.

The paradigm of a triply periodic surface is a triply periodic minimal surface (TPMS)—surface with zero mean curvature. The first example of a TPMS free of self-intersections was introduced by Schwarz in 1865 [8]. It is now known as the Schwarz diamond D surface. Since then strong theoretical arguments of symmetry such as the minimization of the bending energy of the symmetric bilayer supported the picture of such surfaces as the model of the surfactant bilayers. Theoretically the world of self-assembly is almost infinitely rich. Many previously unknown simple and complex periodic structures of cubic symmetry have been found recently in simple Landau-Ginzburg models of ternary mixtures [9]. It is thus very interesting if they are formed in real systems, and how to identify them correctly.

The small-angle x-ray and neutron scattering (SAXS and SANS) experiments (see, for example, [10–12]) are widely used to determine the symmetry and structure of self-assembling systems. The scattering techniques were often used to monitor the structural phase transitions, see, for example, [13,14,3,4]. All these works indicate that the SAXS and SANS are powerful tools that provide information on the symmetry of the structures present in the system. Yet, the x-ray diffraction data are not always conclusive: due to the generally small number of reflections, an accurate reconstruction of an electron or nucleus density map of the cubic cell is often impossible. Even once the space group is rigorously established, there is still the question as to the identity of the minimal surface and thus the topology of the structure. The purpose of this paper is to emphasize this problem. The argument is backed up by scattering spectra of three pairs of cubic structures, Schwarz P and SCN1 of symmetry $Im\bar{3}m$, Schwarz D–diamond and CD ($Pn\bar{3}m$), and Schoen G–gyroid ($Ia\bar{3}d$) and GX6 ($Ia\bar{3}d$), see, Fig. 1. Each pair consists of a well-known simple-cubic structure of a simple topology (small genus) and a complex structure of a large genus both having the same symmetry. The genus is a measure of the topological complexity of the surface. It is the number of its ''handles'' (or ''holes'')–genus of a simple torus with one hole is 1, whereas of a sphere is 0. In the case of TPMS, which as such has an infinite number of handles, the genus is referred to the unit cell with periodic boundary conditions. The simple structures Schwarz P, Schwarz D, Schoen G have the genus of 3, 9, and 5, respectively, while the structures SCN1, CD, and GX6 have genera equal to 43, 73, and 141, respectively [9].

The paper is organized as follows. Section II is devoted to the presentation of the model of the density of the scatterers and numerical methods used in the computation of the scattering intensities. Section III includes the scattering spectra for the latter structures and discussion of the results. Section IV contains the summary.

II. MODEL

The triply periodic minimal surfaces divide the volume into two continuous and separate subvolumes. In surfactant mixtures two physical realizations of a minimal surface are possible. One is a direct phase in which a water film is centered on the surface and surfactant molecules are filling the two subspaces. The second case is an invert phase in which the surface is decorated by a bilayer of surfactant and oil,

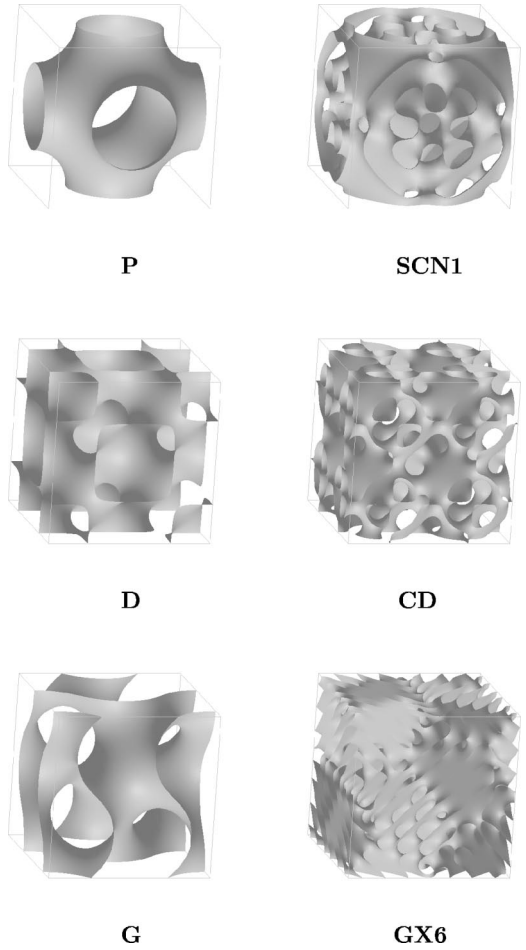

FIG. 1. The zero width mathematical surfaces in the unit cells of the Schwarz P, SCN1, Schwarz D, CD, Schoen G, and GX6 structures. Better pictures of these and many other cubic structures can be seen at http://www.ichf.edu.pl/Dep3.html.

while the two subspaces are filled with water. In our work we focus on the inverted phase.

The two subspaces can be modeled by a concentration field function $f(\mathbf{r})$ taking positive values in one subvolume and negative in the other. Still the fact that the field function takes opposite signs in the two subspaces has no experimental significance but is only related to the mathematical procedure. The condition $f(\mathbf{r})=0$ determines the mathematical surface decorated by the surfactant molecules. The concentration field for structures Schwarz P, SCN1, Schwarz D, CD, Schoen G, and GX6 are taken from the minimization procedure [9]. It is given on a cubic lattice inside a unit cell. Typically the lattice spacing is of the order of 1/50 of the cubic lattice parameter a.

Once we determine values of the field $f(\mathbf{r})$ on the lattice inside the unit cell, we triangulate the surface on which $f(\mathbf{r})=0$. In this way we obtain a set of typically 50 000 triangles covering the whole surface in a unit cell. In real mixtures the surfactant molecule head covers an area of the order of 50 Å^2. The cubic cell parameter is of the order of $a\sim 150$ Å or bigger. In simple structures the surface area per unit cell is of the order of $5a^2$. In more complex ones it is bigger than $10a^2$ [9]. This gives approximately about 10 000 or more of the surfactant molecules per unit cell, which shows that triangles covering the surfaces are small enough to obtain reliable spectra. The scatterers used in computing the scattering intensities are positioned in the middle of each triangle and given the weight equal to the surface area of the triangle. Also each scatterer is associated with a unit vector normal to the surface, which allows us to take into account the effects of the local curvature.

We concentrate on the surface contrast. It is best realized in neutron scattering experiments when the hydrophobic surfactant chains are deuterated. This procedure takes advantage of the very large difference in scattering cross section between the normal hydrogen isotope and deuterium. This is very useful because one can exchange hydrogen with deuterium without altering the structure [15].

If we take $\hat{\rho}(\mathbf{r})$ as the density of the scatterers in the unit cell, the neutron diffraction intensity $I(\mathbf{q})$ is the Fourier transform of the density-density correlation function,

$$I(\mathbf{q})=\langle A(\mathbf{q})A^*(\mathbf{q})\rangle=\int d\mathbf{r}\int d\mathbf{r}'\langle\hat{\rho}(\mathbf{r})\hat{\rho}(\mathbf{r}')\rangle \times\exp[i\mathbf{q}\cdot(\mathbf{r}-\mathbf{r}')]. \tag{1}$$

In a unit cell the density operator $\hat{\rho}$ can be written in the following form:

$$\hat{\rho}(\mathbf{r})=\int d\xi\,\delta(f(\mathbf{r}-\xi\mathbf{n}(\mathbf{r})))\rho_M(\xi). \tag{2}$$

Here $\mathbf{n}(\mathbf{r})$ is a unit vector parallel to the gradient of the field $f(\mathbf{r})$ and $\rho_M(\xi)$ is the molecular density operator equal to

$$\rho_M(\xi)=\theta\left(|\xi|-\frac{L}{2}\right), \tag{3}$$

where L is the width of the hydrocarbon part of the surfactant bilayer. We assume that the $f(\mathbf{r})=0$ surface is located in the middle of the surfactant bilayer. Our model is schematically shown in Fig. 2.

We assume that the multiple scattering of the incident beam in the sample can be neglected. In general, the neutron multiple scattering can be neglected because the Thompson cross section for neutron-nucleus scattering is very small.

The scattering amplitude

$$A(\mathbf{q})=\int d\mathbf{r}\exp[i\mathbf{q}\cdot\mathbf{r}]\hat{\rho}(\mathbf{r}) \tag{4}$$

can be represented by the sum over the points on the surface and the integral along the vectors normal to the surface $\Sigma_{j=1}^{N}s_j\int d\xi$,

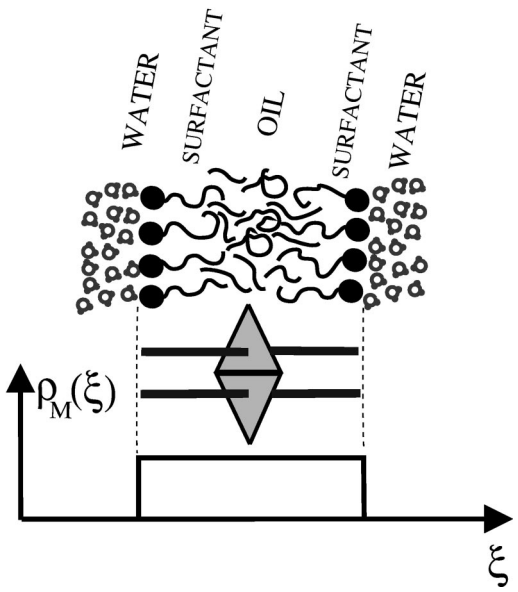

FIG. 2. The schematic representation of the surfactant bilayer and the model. The triangles are obtained from a triangulation of the minimal surface. Then a rod of constant scattering density along its length is positioned in the middle of each triangle in the direction normal to the triangles' surface. Below the model molecular density of scatterers in the bilayer is shown.

$$A(\mathbf{q}) = \sum_{j=1}^{N} s_j \int d\xi' \exp[i\mathbf{q}\cdot(\mathbf{r}_j + \xi'\mathbf{n}_j)] \times \int d\xi \delta(f(\mathbf{r}_j + \xi'\mathbf{n}_j - \xi\mathbf{n}_j))\rho_M(\xi), \tag{5}$$

where s_j is the surface area of the jth triangle and $\mathbf{n}_j$ is a unit vector normal to the surface at the jth point. Please note that the summation over j in Eq. (5) is over the surface given by $f(\mathbf{r})=0$. This point is justified because the total number of scatterers on the surface $f(\mathbf{r})=0$ is the same as on any surface $f(\mathbf{r}-\xi\mathbf{n})=0$ for $|\xi|<L/2$. On a flat surface the surface area $s_j(\xi)$ per one scattering rod is constant and equal to s_j. When the surface bends, the $s_j(\xi)$ is given by the formula $s_j(\xi)=s_j(1+2H\xi+K\xi^2)$ [16], where ξ is negative if the displacement is towards the closest center of curvature, positive otherwise, H is the mean curvature, and K is the Gaussian curvature for $\xi=0$ at the jth point. In this way the surface density of scatterers increases towards the center of curvature and decreases otherwise, but the total number of scatterers remains constant.

Now the amplitude can be rewritten in the following form:

$$A(\mathbf{q}) = \sum_{j=1}^{N} s_j \exp[i\mathbf{q}\cdot\mathbf{r}_j] \frac{\sin\left(\mathbf{q}\cdot\mathbf{n}_j \frac{L}{2}\right)}{\mathbf{q}\cdot\mathbf{n}_j \frac{L}{2}}. \tag{6}$$

And finally, the scattering intensity

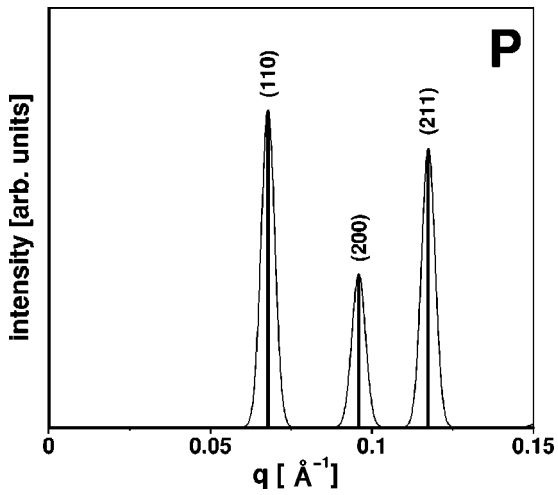

FIG. 3. Scattering spectrum for the Schwarz P structure. The thick solid line represents $\delta\ hkl$ peaks, while the thin line is the convolution of the hkl peaks with the Gaussian resolution function (see text).

$$I(\mathbf{q}) = \left[\sum_{j=1}^{N} s_j \cos(\mathbf{q}\cdot\mathbf{r}_j) \frac{\sin\left(\mathbf{q}\cdot\mathbf{n}_j \frac{L}{2}\right)}{\mathbf{q}\cdot\mathbf{n}_j \frac{L}{2}}\right]^2 + \left[\sum_{j=1}^{N} s_j \sin(\mathbf{q}\cdot\mathbf{r}_j) \frac{\sin\left(\mathbf{q}\cdot\mathbf{n}_j \frac{L}{2}\right)}{\mathbf{q}\cdot\mathbf{n}_j \frac{L}{2}}\right]^2. \tag{7}$$

The influence of the width of the bilayer and the fluctuations have been shown in our previous work [17]. Here, since we do not compute the scattering patterns for any specific surfactant molecule, the width of the hydrocarbon part of the surfactant bilayer has been estimated upon geometrical considerations. We will show the scattering spectra for the structures formed by the surfactant bilayer, which occupies 50% of the volume. This corresponds to the joined volume fraction of oil and surfactant equal to 0.5.

III. RESULTS

All the scattering spectra are in agreement with the space group symmetry of the structures. The prohibited peaks are five to six orders of magnitude smaller then the allowed reflections. The structure factor of these surfaces makes some of the allowed peaks also very weak. This is particularly interesting in the case of the complex structures, where due to this phenomena the low order hkl peaks are small and the intensity is shifted towards the longer scattering vectors and bigger hkl indices.

Figures 3 and 4 present the scattering spectra for two

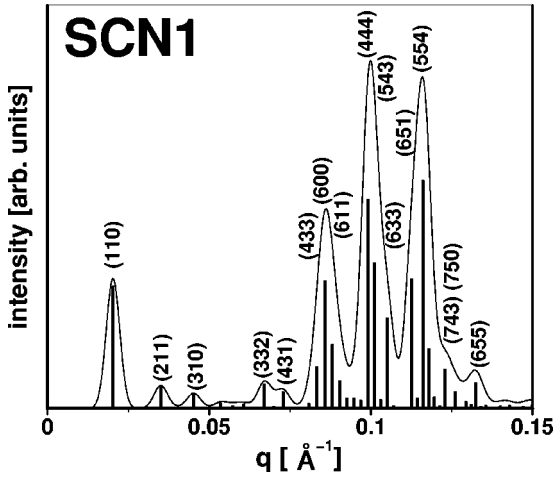

FIG. 4. The scattering pattern for the SCN1 structure (see legend of Fig. 3).

cubic structures of the $Im\bar{3}m$ symmetry. The intensities of the hkl peaks are presented as delta peaks (thick solid line). The figures include also some of the hkl indices corresponding to the underlying peaks. The length of the scattering vector k has been established as follows:

$$q=\frac{2\pi}{a}\sqrt{h^2+k^2+l^2}, \tag{8}$$

where a is the cubic lattice parameter. In all cases we have set the volume occupied by the bilayer to 50% ($\phi_B=0.5$). The volume fraction occupied by the bilayer is a function of the dimensionless width of the bilayer, l_a, expressed as a fraction of the unit cell parameter a. An approximate formula relating these two quantities can be found in [3],

$$\phi_B=s^* l_a+\frac{\pi}{6}\xi_E l_a^3, \tag{9}$$

where s^* is the dimensionless surface area of one unit cell of the minimal base surface and ξ_E is the Euler characteristic given by the expression $\xi_E=2(1-g)$, where g is the genus. In our work we have evaluated the width of the bilayer numerically. Figure 5 presents the volume fraction occupied by the bilayer given by Eq. (9) (dashed line) together with the numerical value (open circles) as a function of the dimensionless width of the bilayer for three different structures.

The bilayer composes of two parallel monolayers of surfactant molecules. A typical length of a surfactant molecule, thus the width of the monolayer is about $10-15$ Å. Assuming that there is also some amount of oil filling the bilayer, we have set the bilayer width to 30 Å. Then the cubic lattice parameter is simply $a=30$ Å$/l_a$. The size of our model Schwarz P structure cell is roughly $a=130$ Å, and for the SCN1 structure $a=440$ Å.

To present typical scattering data that could be obtained in an experiment, we have convoluted the $\delta\, hkl$ peaks with the Gaussian resolution function,

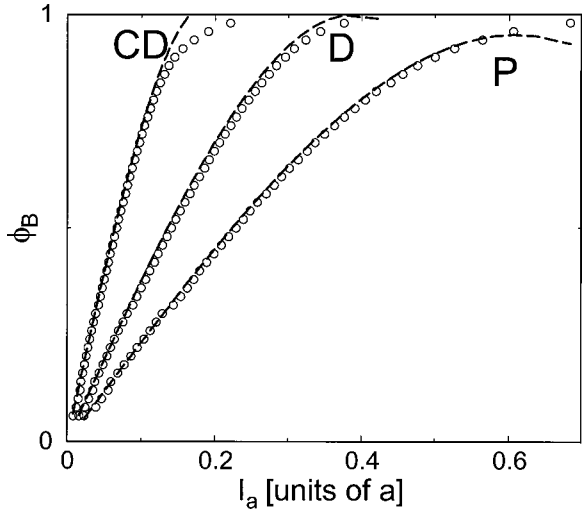

FIG. 5. The volume fraction occupied by the bilayer ϕ_B as a function of the dimensionless width of the bilayer l_a. The analytical approximation is shown by the dashed lines and the numerical values by open circles.

$$R(\mathbf{q})=\frac{1}{\sqrt{2\pi\sigma^2}}\exp\left[\frac{-|\mathbf{q}|^2}{2\sigma^2}\right], \tag{10}$$

where σ is the experimental resolution in inverse angstroms. This way, the experimental intensity can be written as follows:

$$I_{exp}(\mathbf{q})=\frac{1}{\sqrt{2\pi\sigma^2}}\sum_{hkl}\exp\left[\frac{-|\mathbf{q}_{hkl}-\mathbf{q}|^2}{2\sigma^2}\right]I(\mathbf{q}_{hkl}), \tag{11}$$

where $I(\mathbf{q}_{hkl})$ is given by Eq. (7). Since the sum runs over all possible permutations of the hkl indices (including negative values) the function I_{exp} corresponds to a powder diffraction experiment. Yet to reconstruct the experimental intensity profile one should use a more sophisticated function than the Gaussian distribution. Secondly, the intensity is not corrected by the Lorentz-polarization factor since its value depends on the wavelength of the radiation and the type of the detector used in an experiment. Furthermore the relative intensities of the Bragg reflections depend on the width of the bilayer and thus on the composition of the system. Since we present the intensities only for one value of the volume fraction occupied by the bilayer, our aim is only to show general tendencies in the diffraction patterns of simple- and complex-cubic structures. We show what kind of data is experimentally accessible and how much of the information about the structure can be lost due to the experimental setup.

The function $I_{exp}(\mathbf{q})$ for scattering patterns of Schwarz P and SCN1 structures is presented as the thin solid line. We have set the resolution to $\sigma=2\times10^{-3}$ Å^{-1}. This is a reasonable resolution for most synchrotron neutron scattering experiments.

As we see in Fig. 3, the scattering spectrum of the Schwarz P structure is very simple and the peaks are positioned at $q_1=6.8\times10^{-2}$ Å^{-1}, $q_2=\sqrt{2}q_1$, and $q_3=\sqrt{3}q_1$. Thus they can be unambiguously indexed to the simple-cubic symmetry. On the other hand analysis of the scattering spec-

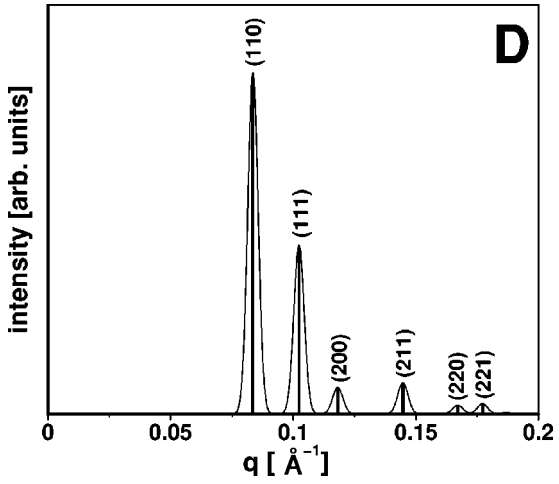

FIG. 6. The scattering pattern for the Schwarz D structure (see legend of Fig. 3). The *hkl* indices should be multiplied by 2 in order to compare them with $Pn\bar{3}m$ space group [18,17].

trum of the complex $Im\bar{3}m$ structure SCN1 proves the opposite. With the established parameters, we observe that some *hkl* peaks merge into a smaller number of bigger peaks. The four most prominent experimental peaks are positioned at $q_1=2\times10^{-2}$ Å^{-1}, $q_2=4.2q_1$, $q_3=5q_1$, and $q_4=6q_1$.

Similar situation can be seen in the $Pn\bar{3}m$ symmetry group. Figures 6 and 7 show scattering spectra for the Schwarz D ($a=210$ Å) and CD ($a=450$ Å) structures, respectively. Please note that in order to compare the *hkl* indices with the $Pn\bar{3}m$ symmetry group, one has to multiply them by a factor 2 [18,17]. In the case of the CD structure, once again the resolution is too small to see distinctive peaks in an experiment. Also in this case the intensity is shifted toward the higher order *hkl* peaks. The situation here is not hopeless thanks to the peak (110), which, like in the SCN1 case, is not extinct by the structure factor. This facilitates approximate extraction of the cubic cell parameters of the

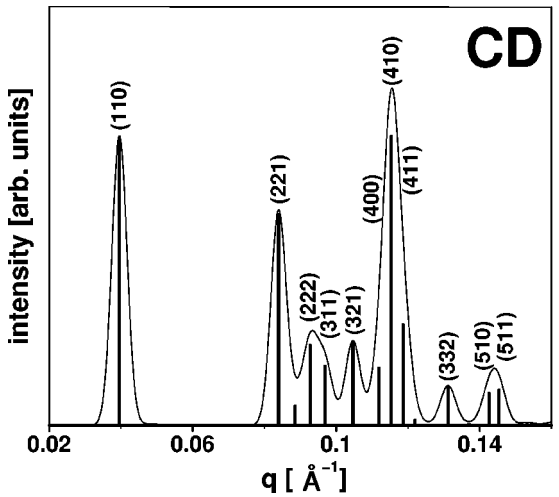

FIG. 7. The scattering pattern for the CD structure (see legend of Fig. 3).

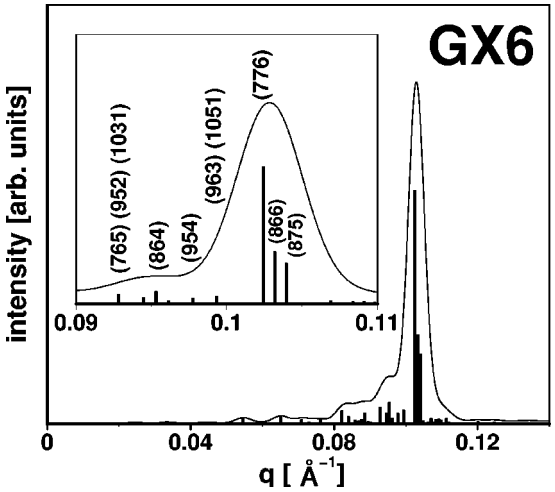

FIG. 8. The scattering pattern for the GX6 structure (see legend of Fig. 3).

SCN1 and CD structures. Still, a much more difficult case is possible as illustrated by the spectrum of the GX6 structure (Fig. 8), where the only experimentally visible peak would be composed of three *hkl* peaks of indices equal to (776), (866), and (875). This peak is located at $q_0=1\times10^{-1}$ Å^{-1}. This one peak would not indicate any cubic symmetry in the system at all. The characteristic length corresponding to this peak $l_{typ}=2\pi/q_0=63$ Å is more then ten times smaller then the real cubic cell parameter ($a=710$ Å). The spectrum of a topologically simple structure Schoen G (Fig. 9), of the same symmetry group ($Ia\bar{3}d$) as the GX6, can be easily indexed to the correct symmetry and does give correct estimates about the size of the unit cell ($a=170$ Å).

A correct determination of the cubic lattice parameter is crucial for the identification of the topology. While the differences in surface area of the bilayer per volume between presented structures are not very big, the differences in surface area per unit cell are large. The quantity $s^*=S/a^2$, where S is the surface area in the unit cell and a is the cubic

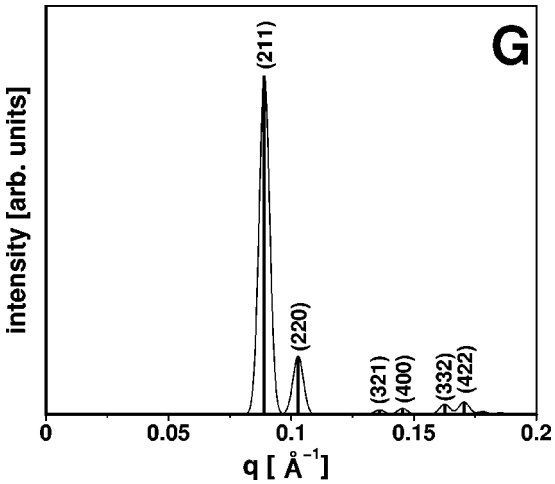

FIG. 9. The scattering pattern for the Schoen G structure (see legend of Fig. 3).

lattice parameter, is a good measure of the topological complexity of the system. For the Schwarz P structure $s^*=2.3$ while for the SCN1 it is over three times bigger; $s^*=7.8$. In the case of other symmetries, the situation is similar; $s^*=3.8$ and 8.1 for Schwarz D and CD, respectively, 3.1 for Schoen G and 12.5 for GX6.

IV. SUMMARY

The list of the experimentally found cubic structures in oil/surfactant/water solutions is long, and progressively new structures are being found. The theoretical models for these structures are triply periodic minimal surfaces, which can be obtained, for example, by minimization of the Landau-Ginzburg free energy [9]. This procedure led to a discovery of large number of different structures. It is still to be established which of these structures are formed in real systems.

We have presented a simple model for obtaining theoretical scattering spectra of TPMS. We have shown that the spectra of the complex structures can be ambiguous. In general, the more topologically complex the structure is, the smaller is the structure factor for the lowest order hkl peaks and the intensity is shifted towards longer scattering wave vectors. This, together with the limitations of the experimental techniques can make it very difficult either to unambiguously prove the existence of these structures or to exclude this possibility.

ACKNOWLEDGMENT

This work has been supported by the KBN Grant No. 2P03B12516.

[1] V. Luzzati and P.A. Spegt, Nature (London) **215**, 701 (1967).
[2] D.C. Turner, Z.G. Wang, S.M. Gruner, D.A. Mannock, and R.N. McElhaney, J. Phys. II **2**, 2039 (1992).
[3] P. Strom and D.M. Anderson, Langmuir **8**, 691 (1992).
[4] P.J. Maddaford and C. Toprakcioglu, Langmuir **9**, 2368 (1993).
[5] S.S. Funari and G. Rapp, J. Phys. Chem. B **101**, 732 (1997).
[6] U. Peter, S. Konig, D. Roux, and A.M. Bellocq, Phys. Rev. Lett. **76**, 20 (1996); **76**, 3866 (1996).
[7] P. Alexandridis, U. Olsson, and B. Lindman, Langmuir **14**, 2627 (1998).
[8] A. H. Schoen, *Infinite Periodic Minimal Surfaces without Self-intersections* (U.S. GPO, Washington, DC, 1970).
[9] W.T. Góźdź and R. Hołyst, Phys. Rev. E **54**, 5 (1996); **54**, 5012 (1996).
[10] P.C. Mason and B.D. Gaulin, Phys. Rev. E **59**, 3 (1999); **59**, 3361 (1999).
[11] R. Gamez-Corrales, J.F. Berret, L.M. Walker, and J. Oberdisse, Langmuir **15**, 6755 (1999).
[12] W.A. Hamilton, P.D. Butler, J.B. Hayter, L.J. Magid, and P.J. Kreke, Physica B **221**, 309 (1996).
[13] P. Barois, D. Eidam, and S.T. Hyde, J. Phys. **C7**, 25 (1990).
[14] M.B. Sjobom, H. Edlund, and B. Lindstrom, Langmuir **15**, 2654 (1999).
[15] B. Svensson, U. Olsson, P. Alexandridis, and K. Mortensen, Macromolecules **32**, 6725 (1999).
[16] S.T. Hyde, J. Phys. **C7**, 209 (1990).
[17] P. Garstecki and R. Holyst, J. Chem. Phys. **113**, 9 (2000); **113**, 3772 (2000).
[18] D.M. Anderson, H.T. Davies, L.E. Scriven, and J.C.C. Nitsche, Adv. Chem. Phys. **77**, 337 (1990); **218**, 1031 (1968).